A Novel Neutral Red Derivative for Applications in High-Performance Red-Emitting Electroluminescent Devices

Pengfei Wang, Zhiyuan Xie, Shiwen Tong, Oiyan Wong, Chun-Sing Lee, Ningbew Wong, Liangsun Hung, and Shuittong Lee*

Center of Super-Diamond and Advanced Films (COSDAF) and Department of Physics and Materials Science, City University of Hong Kong, Hong Kong SAR, China

Received September 9, 2002. Revised Manuscript Received March 5, 2003

A new compound with intramolecular charge transfer (ICT) character—neutral red derivative (**I**)—was designed and synthesized. The new compound is strongly fluorescent in nonpolar and moderately polar solvents. Using this material as a dopant, we fabricated electroluminescent (EL) devices with a structure of indium tin oxide (ITO) coated glass/ *N*,*N*′-bis(1-naphthyl)-*N*,*N*′-diphenyl-1,1′-biphenyl-4,4′-diamine (NPB) (60 nm)/tris(8-hydroxyquinolinato)aluminum (Alq_3):dopant (30 nm)/Alq_3 (20 nm)/Mg−Ag (200 nm). The device showed orange-to-red EL emission with good efficiency and high brightness. The device with a doping concentration of 1 wt % exhibited a high brightness of 18400 cd/m^2 at a driving voltage of 13 V, and the current efficiency is 5.2 cd/A at a current density of 20 mA/cm^2. An important feature of the device is its fairly constant current efficiency over a wide range of current density from 1 mA/cm^2 to as high as 500 mA/cm^2 at different doping concentrations. The current devices show obvious advantages over many reported red-emitting OLEDs, which show significant drops in efficiency as the current density and/or dopant concentration increases. The present red dopant is particularly suitable for passive-matrix display applications where a high excitation density is required.

I. Introduction

Organic light-emitting devices (OLEDs) have received much attention because of their potential applications in flat-panel displays.[1−4] Since the initial works on high-efficiency OLEDs,[5,6] many research efforts have focused on the development of full-color displays. For full-color applications, it is essential to have RGB (red−green−blue) materials with good color purity and high efficiency. After extensive studies in the past decade, efficient blue and green materials have been developed to meet the requirement of commercial OLED applications. However, there is still a lack of red materials with good color purity, high efficiency, and good stability. Many known and new red fluorescent dyes have been tried[7−9] and more recently some red phosphorescence dyes have also been introduced.[10−12] Among these, one prominent example is the development of 4-(dicyanomethylene)-2-*tert*-butyl-6-(1,1,7,7-tetramethyljulolidyl-9-enyl)-4*H*-pyran (DCJTB), which is arguably the state-of-the-art red dopant, by modifying the well-known laser dye 4-(dicyanomethylene)-2-methyl-6-(*p*-dimethylaminostyryl)-4*H*-pyran (DCM). However, for OLEDs doped with DCJTB, device efficiency and color purity are usually traded and compromised.[7,8] For rare-earth complexes, the color purity is excellent, but the efficiency and chemical stability is much below the requirement of commercial applications.[13] Recently, triplet emitters have been developed to obtain very efficient red devices.[14] However, due to the long lifetime of the triplet state, the density of the triplet state can be more easily saturated for high-brightness applications. As a result, the efficiency of triplet red emitter usually decreases very quickly as brightness increases.[10−12] This will pose a potential problem for applications requiring high excitation density such as in passive dot-matrix displays. Thus, new high-performance red dyes are still much in demand.

Neutral red and its derivatives are a kind of the phenazine dyes, which are widely used as pH sensors and biological stains in biology[15−17] as well as sensitizers

* To whom correspondence should be addressed. E-mail: apannale@cityu.edu.hk. Fax: +852-27844696. Tel: +852−27889606.

(1) Chen, C. H.; Shi, J.; Tang, C. W. *Macromo. Symp.* **1997**, *125*, 1.
(2) Shirota, Y. *J. Mater. Chem.* **2000**, *10*, 1.
(3) Segura, J. L. *Acta Polym.* **1998**, *49*, 319.
(4) Mitschke, U.; Bauerle, P. *J. Mater. Chem.* **2000**, *10*, 1471.
(5) Tang, C. W.; VanSlyke, S. A. *Appl. Phys. Lett.* **1987**, *51*, 913.
(6) Burroughes, J. H.; Bradley, D. D. C.; Brown, A. R.; Marks, R. N.; Mackay, K.; Friend, R. H.; Burns, P. L.; Holmes, A. B. *Nature* **1990**, *347*, 539.
(7) Chen, C. H.; Tang, C. W.; Shi, J.; Klubek, K. P. *Thin Solid Films* **2000**, *363*, 327.
(8) Chen, B. J.; Lin, X. Q.; Cheng, L. F.; Lee, C. S.; Gambling, W. A.; Lee, S. T. *J. Phys. D: Appl. Phys.* **2001**, *34*, 30.
(9) Picciolo, L. C.; Murata, H.; Kafafi, Z. H. *Appl. Phys. Lett.* **2001**, *78*, 2378.
(10) O'brien, D. F.; Baldo, M. A.; Thompson, M. E.; Forrest, S. R. *Appl. Phys. Lett.* **1999**, *74*, 442.
(11) Adachi, C.; Baldo, M. A.; Forrest, S. R. *J. Appl. Phys.* **2000**, *87*, 8049.
(12) Adachi, C.; Baldo, M. A.; Forrest, S. R.; Lamansky, S.; Thompson, M. E.; Kwong, R. C. *Appl. Phys. Lett.* **2001**, *78*, 1622.
(13) Kido, J.; Nagai, K.; Okamato, Y.; Skothheim, T. *Chem. Lett.* **1991**, 1267.
(14) Baldo, M. A.; Adachi, C.; Forrest, S. R. *Phys. Rev. B* **2000**, *62*, 10967.

10.1021/cm0209214 CCC: $25.00
Published on Web 04/05/2003

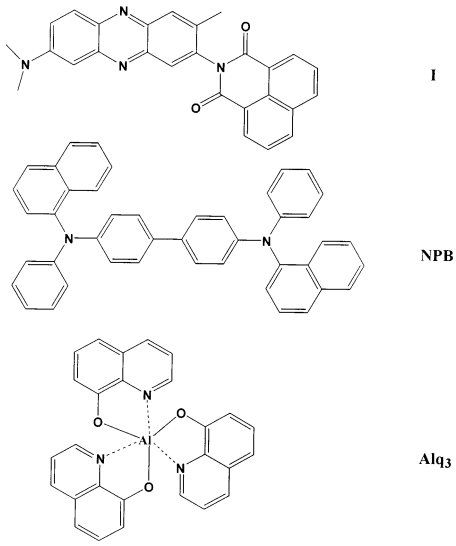

Figure 1. Molecular structures of compounds used in EL devices.

for solar cells.[18] Most neutral red derivatives are strongly fluorescent in longer wavelength (orange−red region). Therefore, it is of interest to explore neutral red derivatives for potential applications in OLEDs. In the present work, we investigated the spectral and photophysical behaviors of a novel neutral red derivative (shown in Figure 1) with intramolecular change transfer (ICT) property. The electroluminescent (EL) performance of the compound as a dopant in OLED was evaluated. Orange-to-red emitting devices with high brightness and good performance were obtained.

II. Experimental Section

Materials. All solvents used for the synthesis of the neutral red derivative were at least of reagent-grade quality and were used without further purification. Solvents for spectroscopic determinations were of spectroscopic grade and were used without further purification. Neutral red and 1,8-naphthalic anhydride (Acros Organics) were used as received. *N*,*N*′-bis-(1-naphthyl)-*N*,*N*′-diphenyl-1,1′-biphenyl-4,4′-diamine (NPB) and tris(8-hydroxyquinolinato)aluminum (Alq_3) were prepared by general methods and purified by train sublimation before use.

Spectroscopic Measurements. ^{1}H NMR spectra were measured on a 300-MHz Varian Gemini spectrometer. Mass spectrometry (MS) was performed on a PE SCIEX LC/MS spectrometer. Elemental analyses were done on a Vario EL Elementar. UV−visible absorption spectra were recorded on a Perkin-Elmer Lambda 2S UV−visible spectrophotometer. Fluorescence spectra were obtained using a Perkin-Elmer LS-50 fluorescence spectrophotometer. Fluorescence quantum yields (Φ_f) in different solvents at room temperature were measured by referencing to a methanol solution of Rhodamine B as a standard ($\Phi_f = 0.65$),[19] with corrections made for differences in the refractive indices of solvents.[20] The absorbance at the excitation wavelength was <0.1 to prevent the "inner filter effect". Electron energy levels of various compounds were measured using ultraviolet photoelectron spectroscopy (UPS) and UV−visible optical absorption spectroscopy.

Device Fabrication and Characterization. EL devices fabricated in this work had a configuration of indium tin oxide (ITO) coated glass/NPB (60 nm)/Alq_3:dopant (30 nm)/Alq_3 (20 nm)/Mg−Ag (200 nm). In this structure, *N*,*N*′-bis(1-naphthyl)-*N*,*N*′-diphenyl-1,1′-biphenyl-4,4′-diamine (NPB) was used as the hole-transporting material and tris(8-hydroxyquinolinato)-aluminum (Alq_3) as the host and electron-transporting material. ITO-coated glasses with a sheet resistance of 30 Ω/□ were used as the substrate and anode. All the organic layers and metallic cathode Mg:Ag (10:1) were successively deposited onto the ITO glass at a vacuum of 3×10^{-6} mbar. The rate of deposition for the organic layers and metallic cathode were 0.2 and 0.5 nm/s, respectively. The emission area of the devices was 10 mm^2. The EL spectra and luminance−current density−voltage characteristics of devices were measured by using a SpectraScan PR650 spectrophotometer and a computer-controlled voltage−current source, Keithley 236, under the ambient condition.

Synthesis of Neutral Red Derivative (I). Neutral red (0.25 g) and 0.2 g of 1,8-naphthalic anhydride were suspended in 20 mL of quinoline. The mixture was refluxed for 24 h at 220 °C under nitrogen. After cooling, the solution was poured into 50 mL of ethanol. A red precipitate was collected and purified by re-crystallization from ethanol; after drying 0.32 g of deep red needle was obtained.^{1}H NMR (300 MHz, $CDCl_3$): δ 2.43 (s, 3H), 3.23 (s, 6H), 7.07 (d, $J = 3.0$ Hz, 1H), 7.62−7.65 (m, 1H), 7.83−7.88 (m, 2H), 8.01−8.15 (m, 3H), 8.33−8.36 (m, 2H), 8.71−8.74 (m, 2H). MS: (*m*/*e*) 433 ($M^+ + 1$). Anal. Calcd for $C_{27}H_{20}N_4O_2$: C, 74.98; H, 4.66; N, 12.96. Found: C, 74.83; H, 4.85; N, 12.79.

III. Results and Discussion

Molecular Structure. From the molecular structure of compound **I** (Figure 1), it is clear that dimethylamino moiety at the 8-position acts as an electron-donating group, and quinoxaline ring and naphthalic anhydride imide act as electron acceptors. The electron-donating group $-NH_2$ in the neutral red molecule is substituted by an electron-withdrawing group, naphthalic anhydride imide. As a result, the emission wavelength is expected to shift to red due to enhanced intramolecular charge transfer in the excited state. On the other hand, this compound also belongs to the fused heterocyclic aromatic ring analogue. From the viewpoint of molecular engineering for design of highly fluorescent molecules, such a combination of structural characteristics will generally lead to the following advantages: (i) a high fluorescence quantum yield due to the suppression of the "proximity effect"[21] from the interaction of both $n\pi$ and $\pi\pi$ electron configurations and internal conversion decay from the free rotation of unbridged double bond;[22] (ii) a large Stokes' shift, especially in the solid state; (iii) a relatively narrow emission band resulting from the reduced vibration due to the bridged structure of the molecule.

Spectral, Photophysical Behaviors and Energy Levels. Table 1 lists the absorption maxima and molar extinction coefficients of compound **I** in a variety of solvents. A red shift in the absorption maxima was observed with increasing solvent polarity, indicating

(15) Faraggi, M.; Peretz, P.; Rosenthal, I.; Weinraub, D. *Chem. Phys. Lett.* **1984**, *103*, 310.
(16) Dierickx, P. J.; Scheers, E. M. *J. Appl. Toxicol.* **2002**, *22*, 61.
(17) Huang, C. Z.; Li, Y. F.; Feng, P. *Talanta* **2001**, *55*, 321.
(18) Jana, K.; Bhowmik, B. B. *J. Photochem. Photobiol. A: Chem.* **1999**, *122*, 53.
(19) Arbeloa, I. L.; Rohatgi-Mukherjee, K. K. *Chem. Phys. Lett.* **1986**, *129*, 607.
(20) Lakowicz, J. R. *Principles of Fluorescence Spectroscopy*; Plenum: New York, 1985; Chapters 3 and 5.
(21) Siebrand, A., Jr.; Zgierski, M. Z. *J. Chem. Phys.* **1980**, ***72***, 1641.
(22) (a) Caldwell, R. A.; Carlcacci, L.; Doubleday, C. E., Jr.; Furlanni, T. R.; King, H.; McIver, J. W., Jr. *J. Am. Chem. Soc.* **1988**, *110*, 6901. (b) Wang, P.; Wu, S. *J. Photochem. Photobiol. A: Chem.* **1995**, *86*, 109.

Table 1. Spectral and Photophysical Data of Compound I at Room Temperature

solvents:	*n*-heptane	DCM[a]	AN[b]	MeOH
$E_T(30)$ (kcal/mol):	30.8	41.1	46.0	55.5
$\lambda_{max}^{ab.}$ (nm)	458	484	488	502
ϵ ($dm^3\,mol^{-1}\,cm^{-1}$)	15230	16060	14980	17020
$\lambda_{max}^{em.}$ (nm)	508	569	590	592
Φ_f	~1	0.75	0.35	0.12

[a]DCM: dichloromethane. [b] AN: acetonitrile.

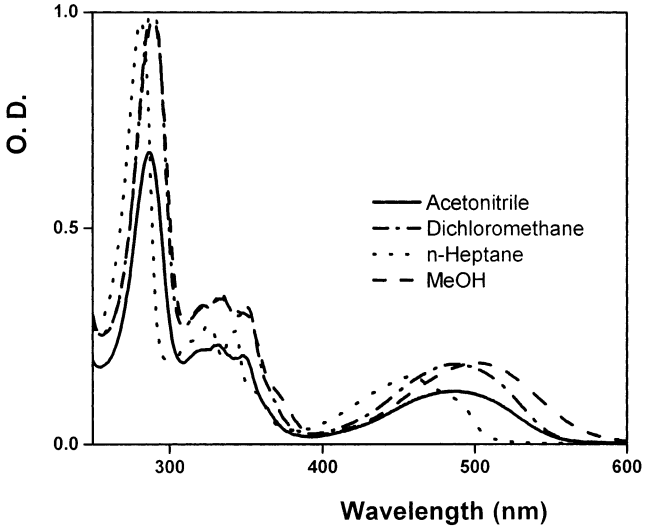

Figure 2. Normalized absorption spectra of compound **I** in different solvents (M = 1 × 10^{-5} mol/L): (—) acetonitrile; (— - —) dichloromethane; (- - -) *n*-heptane; (— —) methanol.

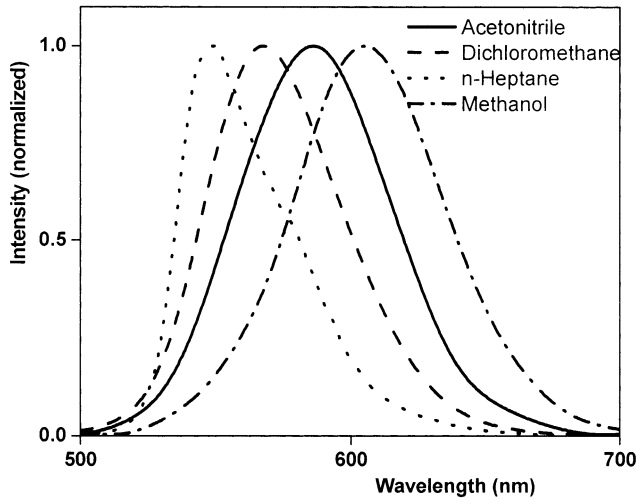

Figure 3. Normalized fluorescence spectra of compound I in different solvents: (—) acetonitrile; (— - —) dichloromethane; (- - -) *n*-heptane; (— —) methanol; $\lambda_{ex.}$ = 480 nm.

that this molecule exhibits intramolecular charge transfer character in the ground state (Figure 2). The fluorescence spectra of compound **I** in different solvents are shown in Figure 3. The fluorescence maximum is dramatically shifted to the red from 508 nm in a nonpolar solvent—*n*-heptane—to 590 nm in a strongly polar solvent—acetonitrile. Since neither solvent nor solute may rearrange during the course of electronic transition, any solvent stabilization of the ground state is revealed by a shift in the absorption spectrum. Similarly, the solvent stabilization of the excited state is revealed by a shift in fluorescence spectrum. A larger

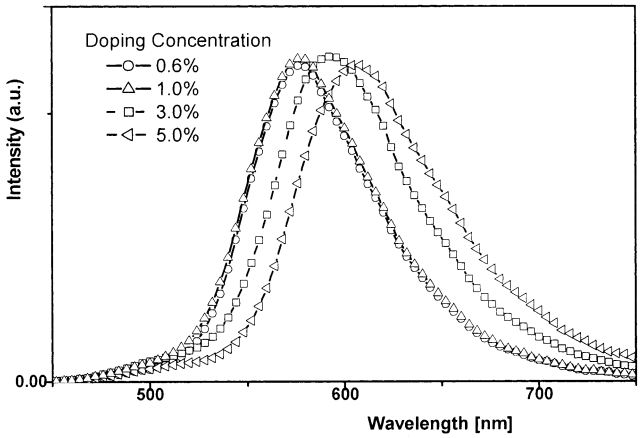

Figure 4. Normalized electroluminescence spectra of devices at different doping concentrations. Structure: ITO-coated glass/NPB (60 nm)/Alq_3:dopant (30 nm)/Alq_3 (20 nm)/Mg—Ag (200 nm).

solvent-induced shift in the fluorescence as compared to the shift in UV—vis absorption spectra was observed due to the stronger interaction between the molecules in the singlet excited state and surrounding solvents. The fluorescence quantum yields of compound **I** in different solvents are also listed in Table 1. The values reveal a significant dependence on the solvent polarity, for example, $E_T(30)$.[23] The fluorescence quantum yield of compound **I** decreases from almost unity in a nonpolar solvent—*n*-heptane—to 0.35 in a strongly polar solvent—acetonitrile. This result indicates a strong ICT character of the molecule in the excited state. The lower fluorescence quantum yield in a proton solvent—methanol—can be attributed to the hydrogen bond interaction between the molecule and surrounding solvent, which results in additional nonradiative decay.

The ionization potential (IP) of compound **I** was measured by UPS, and the electron affinity (EA) was estimated from the IP value and the band gap, which is generally obtained from the edge of the absorption spectrum. The IP and EA of compound **I** are 5.4 and 3.2 eV, respectively. As these values are bracketed by the IP and EA values of Alq_3 (IP = 5.62, EA = 2.85 eV),[24] Alq_3 was chosen as the host for compound **I** in the OLEDs, and an efficient energy transfer might be expected in this host—guest system.

Electroluminescent Performance. Since compound **I** shows a strong emission in solution, it is worth investigating its electroluminescent behavior as a dopant in EL devices. Multilayer EL devices with NPB as the hole-transporting material and Alq_3 as the host and electron-transporting material were fabricated and characterized. Figure 4 shows the EL spectra of devices at different doping concentrations from 0.6 to 5 wt %. The emission spectra shift from orange ($\lambda_{max.}$ = 576 nm) to red ($\lambda_{max.}$ = 608 nm) with increasing doping concentration, showing the typical behavior of donor—acceptor (D—A) compounds. The reason can be attributed to a change in the polarity of the surrounding medium caused by the increase of the highly polar excited molecules.[25] The results are consistent with that ob-

(23) Reichardt, C. *Angew. Chem., Int. Ed. Engl.* **1979**, *18*, 98.
(24) Hamada, Y.; Kanno, H.; Takahashi, T.; Usuki, T. *Appl. Phys. Lett.* **1999**, *75*, 1682.

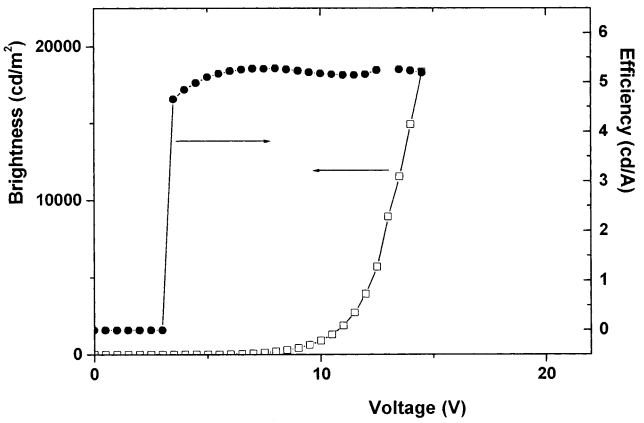

Figure 5. Efficiency−luminance−voltage characteristics of a 1.0 wt % doped device. Structure: ITO-coated glass/NPB (60 nm)/Alq_3:dopant (30 nm)/Alq_3 (20 nm)/Mg−Ag (200 nm).

served in solution for compound **I** in which a bathochromic shift in emission spectra was found with increasing solvent polarity. The feature of tunable emission color can be applied to optimize the emission of EL devices by a method so called "solid-state-solvation effect" (SSSE).[26] Furthermore, the device also shows a relatively narrow emission band with a full-width at half-maximum (fwhm) of 75−80 nm, which is narrower than those (fwhm >100 nm) of typical DCM series dyes,[25−28] such as DCM, DCM2, DCJT, and DCJTB. This is probably due to the bridged structure between the donor and acceptor in this molecule, resulting in reduced vibration, while the double bond is unbridged in the case of DCM series dyes. The efficiency−luminance−voltage characteristics of the device with compound **I** as an emitting material are shown in Figure 5. It reveals that the devices based on compound **I** show very bright orange-to-red emission with high efficiencies at low doping concentrations. Both luminance and efficiency decrease with increasing doping concentration, probably due to the aggregation at high concentration, which results in additional nonradiative decay processes of the excited states (Figure 6, 7). More detailed EL performances for devices based on compound **I** are listed in Table 2. For example, a device with doping concentration of 1 wt % shows good performance with a high luminance of 18400 cd/m^2 at 13 V, a low turn-on voltage of 3.5 V, and a good efficiency of 5.2 cd/A. In addition, Figure 7 shows that the current efficiencies remain almost flat over a wide range of drive current densities from 1 mA/cm^2 to as high as 500 mA/cm^2 at different doping concentrations while the luminance increases concomitantly. This is particularly important for the passive-matrix displays, which require a high excitation density.

In conclusion, a new neutral red derivative was designed and synthesized, and its spectral and photophysical properties were studied. Using this strongly fluorescent compound as a dopant, EL devices with a structure of indium tin oxide (ITO) coated glass/NPB (60 nm)/Alq_3:dopant (30 nm)/Alq_3 (20 nm)/Mg−Ag(200 nm) show bright orange-to-red emission with high efficiencies and relatively narrow emission bands. The tunable emission wavelength can be applied to fabricate devices with different colors, especially white-emitting OLED, by the SSSE method, similar to the work of Thompson and Forrest on DCM series dyes.[26] Another attractive feature for the current device is that its current efficiency remains almost constant over a wide range of current densities from 1 mA/cm^2 to as high as 500 mA/cm^2 at varying doping concentrations, which is

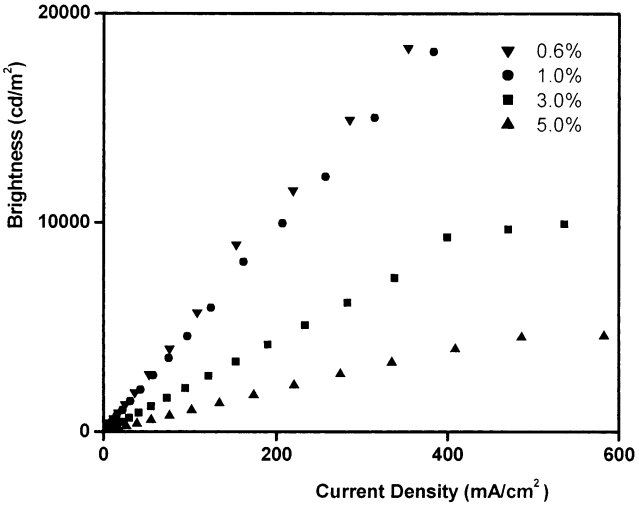

Figure 6. Efficiency−current density characteristics of an ITO-coated glass/NPB (60 nm)/Alq_3:dopant (30 nm)/Alq_3 (20 nm)/Mg−Ag (200 nm) device at different doping concentrations.

Table 2. EL Performances of Compound I-Doped Devices with the Structure of NPB (60 nm)/Alq_3:Dopant (25 nm)/Alq_3 (30 nm)

doping concentration (wt %)	$\eta^{max.}$ (cd/A)	devices performance at 20 mA/cm^2		
		L (cd/m^2)	η (cd/A)	λ (nm)
0.6	5.0	1040	5.0	576
1.0	5.3	1200	5.2	576
3.0	2.4	470	2.4	592
5.0	1.0	230	1.0	608

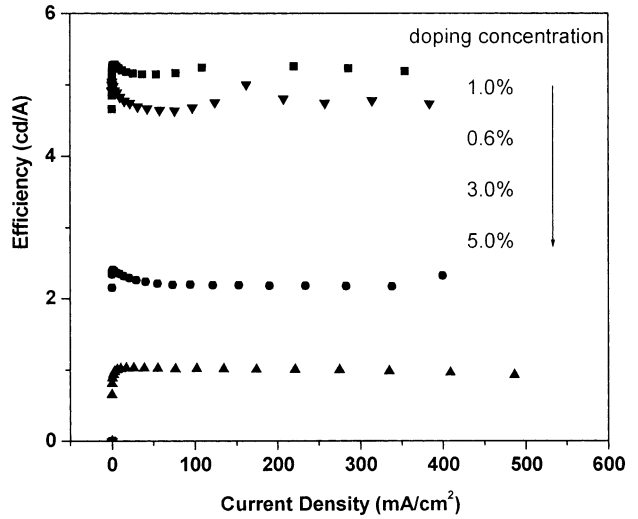

Figure 7. Brightness−voltage characteristics of an ITO-coated glass/NPB (60 nm)/Alq_3:dopant (30 nm)/Alq_3 (20 nm)/Mg−Ag (200 nm) device at different doping concentrations.

(25) Bulovic, V.; Shoustikov, A.; Baldo, M. A.; Bose, E.; Kozlov, V. G.; Thompson, M. E.; Forrest, S. R. *Chem. Phys. Lett.* **1998**, *287*, 455.
(26) Bulovic, V.; Deshpande, R.; Thompson, M. E.; Forrest, S. R. *Chem. Phys. Lett.* **1999**, *308*, 317.
(27) Tang, C. W.; Van Slyke, S. A.; Chen, C. H. *J. Appl. Phys.* **1989**, *65*, 3610.
(28) Chen, C. H.; Tang, C. W.; Shi, J.; Klubek, K. P. *Macromol. Symp.* **1997**, *125*, 49.

particularly desirable for the passive-matrix display application. This work suggests that compounds with the combined structure of a bridged double bond in the ring and ICT character in the molecule can be strongly emissive and are promising dopants in OLEDs. Moreover, the present series of compounds may be modified to shift the emission wavelength, for example, by simply substituting dimethylamino with a sterically hindered, stronger electron-donating group such as the tetramethyljuloline group similar to the modification of DCM into DCJTB.[28]

Acknowledgment. This work is supported by the Research Grants Council of Hong Kong SAR (Project No. N_CityU 114/00).

CM0209214